Materials Chemistry and Physics 132 (2012) 529–533

Contents lists available at SciVerse ScienceDirect

Materials Chemistry and Physics

journal homepage: www.elsevier.com/locate/matchemphys

Stabilization of polyaniline by the incorporation of magnetite nanoparticles

Beatriz E. Jaramillo-Tabares [a], Franklin Jaramillo Isaza [a,*], Susana I. Córdoba de Torresi [b]

[a] Corrosion and Protection Group, Center for Research, Innovation and Development of Materials-CIDEMAT, Universidad de Antioquia, Medellín, Colombia
[b] Instituto de Química, Universidade de São Paulo, C.P. 26077, 05513-970 São Paulo (SP), Brazil

ARTICLE INFO

Article history:
Received 26 July 2011
Received in revised form
15 November 2011
Accepted 24 November 2011

Keywords:
Polyaniline
Magnetite
Nanocomposites
Redox interactions

ABSTRACT

Nanocomposites obtained from the polymerization of aniline in the presence of nanoparticles of magnetite (Fe_3O_4) have been investigated in previous studies. However, there is a lack of information available on the redox interaction of the nanoparticle/conductive polymer couple and the stability that such an oxide can give to the organic phase. In this work, Fe_3O_4 nanoparticles were incorporated into a PANi matrix by the in-situ oxidative polymerization method. A combination of X-ray diffraction, Mössbauer spectroscopy, transmission electronic microscopy, UV–visible spectroscopy as well as the cyclic voltammetric and Raman spectroscopy techniques, was used to understand the redox effect that the partially oxidized nanoparticles produced on the polymer. It was found that magnetite greatly stabilised PANi, mainly by enhancing the Leucoemeraldine/Emeraldine redox couple and also by reducing the bipolaronic state.

1. Introduction

Polyaniline (PANi) is one of the most studied conducting polymers due to its unique electronic and optical properties, excellent environmental stability and good processability. It has been widely investigated in the last decade as a result of the aforementioned properties and its excellent performance in applications such as conductive polymers in sensors, conductive separation membranes, antistatic devices and corrosion control, among many others [1–8]. Its structure consists of two segments: a flat structure of two imine groups and a quinoid ring, and tetrahedral segments of two amine groups separating three benzenoid rings. The structure can be readily modified upon protonation. Fig. 1 shows the different forms of PANi and its transformation by either acid/base or electrochemical reactions [9]. PANi has been modified by the incorporation of nanoparticles to improve its electrical properties and to design novel nanocomposites with functional properties. However, stability in air is one of the main problems of conductive polymers and is one which has not yet been solved.

Magnetite (Fe_3O_4) is an iron oxide semiconductor that has an inverse spinel structure, with a face-centered cubic unit cell based on 32 O^{2-} ions that contain 8 Fe^{3+} ions on the tetrahedral sites (A sites) and 16 Fe^{3+} ions on the octahedral sites (B sites); 8 of which are Fe^{2+} and the other 8 are Fe^{3+}. Its formula can be written as $Fe^{3+}[Fe^{2+}\ Fe^{3+}]O_4$, where the brackets denote octahedral sites. Iron oxides offer a series of magnetic and electronic characteristics that combined with PANi produce magnetic polymer nanocomposites, a new class of functional materials with immense potential for application in cell separation, enzyme immunoassay, drug targeting, electromagnetic devices and electromagnetic interference suppression [11–13].

Papers have been published [14–21] regarding the magnetic and conducting properties of PANi based nanocomposites containing several metals ions and nano-oxides. Such functional nanoparticles include magnetite [14,15]. However, the electrical/electronic interaction of the polymer/nano-oxide pair, which is ultimately responsible for the excellent performance of nanocomposites, is not yet clear. Umare et al. [16] found that the discharge capacity of the aqueous Zn/PANi battery was improved by the incorporation of Fe_3O_4 nanoparticles into the polymer backbone. This is due to the synergic effect resulting from the combination of inorganic material and the polymer. Similar results have been found by other researchers [17,21]. In our previous work, the influence of Fe_3O_4 on several properties of polypyrrole (PPy) was demonstrated. The presence of Fe_3O_4 in the polymer matrix was shown to decrease the oxidation process of the polymer, stabilizing its conductivity and giving a clear indication of redox interactions between Fe_3O_4 and polypyrrole [22].

In the study presented here, aniline was polymerized in the presence of Fe_3O_4 nanoparticles. The resulting nanocomposites were characterized by TEM, XRD and Mössbauer spectroscopy to confirm the formation of the Fe_3O_4/PANi nanocomposite. Furthermore, combined UV–visible spectroscopy and cyclic voltammetric experiments were then carried out to study possible polymer transformations. Raman Spectroscopy was also conducted to characterize the resulting nanocomposites. From the obtained results it

* Corresponding author. Tel.: +57 4 2196680.
E-mail address: franklinj@udea.edu.co (F.J. Isaza).

0254-0584/$ – see front matter © 2011 Elsevier B.V. All rights reserved.
doi:10.1016/j.matchemphys.2011.11.065

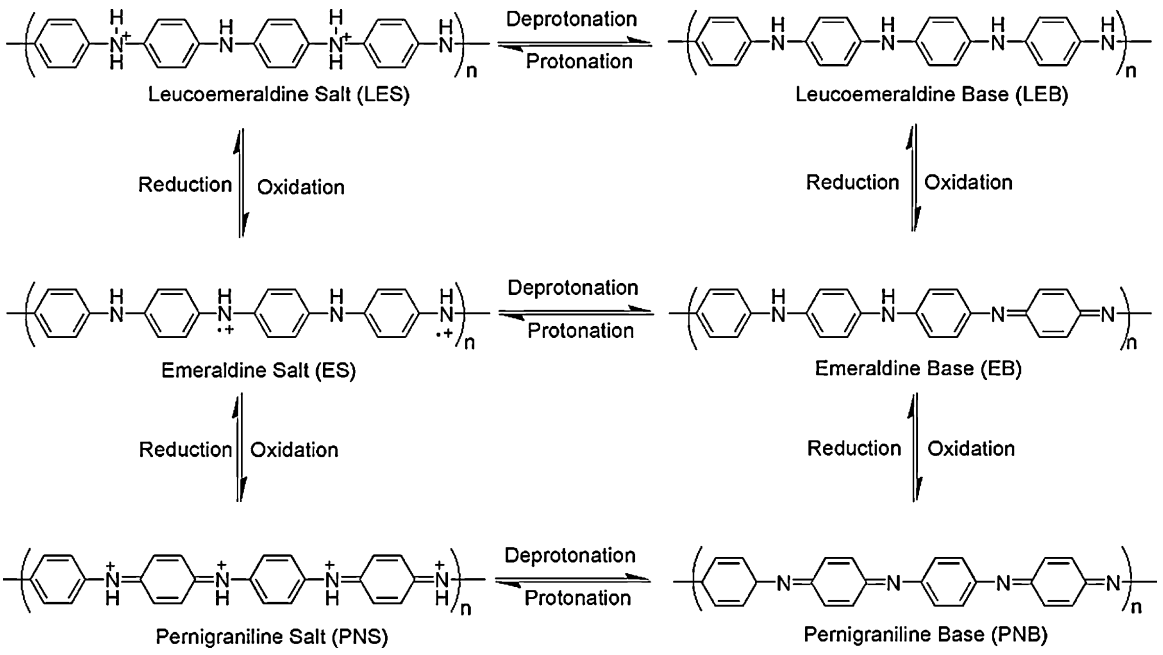

Fig. 1. Polyaniline chemical structures at different redox states [10].

is possible to conclude that Fe_3O_4 nanoparticles have a remarkable redox effect on the conducting polymer by stabilizing the reduced PANi form.

2. Materials and methods

2.1. Synthesis of Fe_3O_4 nanoparticles

Magnetite nanoparticles were prepared by the hydrothermal-oxidation method in accordance with the literature [23–25], with few modifications and following a typical procedure, as described below. A solution mixture of $NaNO_3$ and NaOH was placed in a 1000 mL glass reactor; the mixture was stirred under nitrogen for 45 min, followed by dropwise addition of aqueous solution containing $FeCl_2$ and polyethylene glycol (PEG) as a dispersant. The reaction was allowed to proceed for 2 h at 70 °C at pH 9. The resulting magnetic fluid was dialyzed and purified repeatedly from ionic species.

2.2. Synthesis of PANi/Fe_3O_4 nanocomposites

Nanocomposites were prepared via an in-situ polymerization of aniline in an aqueous solution containing Fe_3O_4 magnetic fluid and PEG. The polymerization was carried out in a 500 mL round-bottomed flask immersed in an ultrasonic bath for 2 h at 0–5 °C. Ammonium persulphate was used as an oxidant agent. The products were purified by magnetic separation, a procedure that was repeated four times. The particles were then immersed in 0.2 M of HCl aqueous solution for 48 h to remove non-encapsulated Fe_3O_4 particles. Magnetic separation phases and washing with distilled water were repeatedly carried out [26]. The nanocomposite was washed out with 0.1 M NH_4OH until the filter was colorless and left under stirring in 0.1 M NH_4OH solution for 5 h to finally be converted into emeraldine base nanocomposite. The product was filtered and washed with deionized water until the filtrate was neutral. The nanocomposites were dried under vacuum at 40–50 °C for a period of 3 days and then stored in a desiccator at room temperature prior to analysis. PANi/Fe_3O_4 composites with approximately 2% of Fe_3O_4 were obtained.

2.3. Characterization

The nanocomposites were characterized by X-Ray diffraction, Mössbauer spectroscopy, transmission electron microscopy, UV–visible spectroscopy, cyclic voltammetry and Raman spectroscopy. The X-ray diffractograms were recorded on a Rigaku D-MAX-III/B model X-ray diffractometer using copper Kα radiation. Mössbauer spectroscopy was employed in transmission mode at room temperature with a source of ^{57}Co immersed in an Rh matrix. TEM images ware recorded with a JEOL FX 2000 II microscope. UV–vis experiments were performed in a Varian Cary 5000 UV–vis–NIR spectrophotometer. The cyclic voltammetry (CV) curves were obtained in 0.1 M H_2SO_4 aqueous solution by using an IM6e BASS-ZANHER Potenciostat instrument. Raman spectra were recorded on a Renishaw Raman imaging microscope (System 3000), connected to a CCD detector (Wright, 600 × 400 pixels), using 632.8 nm excitation radiation (He–Ne laser-Spectra Physics, model 127). CV and UV–vis were carried out for 0, 2, 7 and 18 days for samples left in air at room temperature.

3. Results and discussion

Fig. 2 shows the characteristic diffraction peaks of Fe_3O_4 nanoparticles (18.32°, 30.08°, 35.44°, 37.04°, 43.12°, 53.48°, 56.94°, 62.58°, 71°, 74.04°, 78.84°) after being analyzed using the MAUD software [25], and taking the cell parameters from the literature [27,28]. The calculated crystallographic parameters are shown in Table 1.

The small differences for the two magnetite samples are within experimental error. Taking into account the easy transformation of magnetite (Fe_3O_4) into maghemite (γ-Fe_2O_3) in air at room temperature, there is a lack of information in the literature about the

Table 1
Cell parameters for Fe_3O_4 and PANi/Fe_3O_4.

Sample	Phases fitted	Cell parameters (Å)	Crystallite size (nm) ±1.8
Fe_3O_4	Magnetite	8.38	79.4
PANi/Fe_3O_4	Magnetite	8.37	83.4

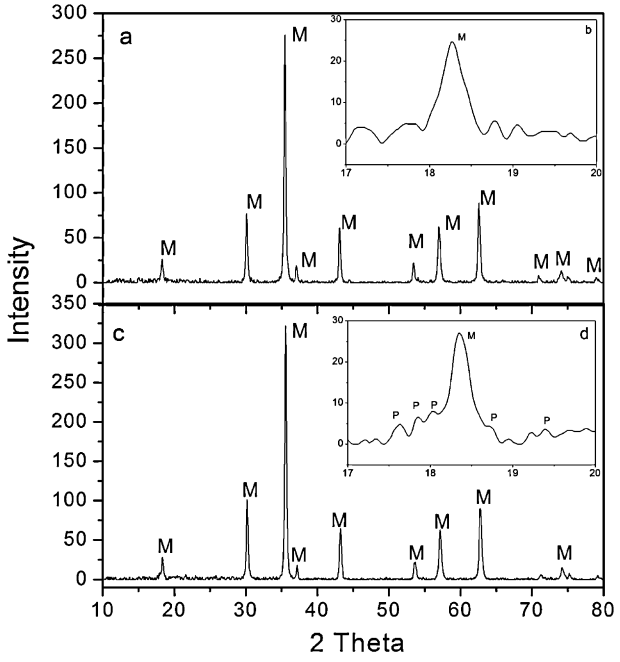

Fig. 2. X-ray diffractograms. (a) Fe_3O_4, (b) Fe_3O_4 zoom, (c) Fe_3O_4/PANi nanocomposites, (d) Fe_3O_4/PANi zoom. M = magnetite, P = Polyaniline.

purity of the reported nanocomposites. In this study, XRD results confirmed the presence of unmodified magnetite in the nanocomposites.

The higher crystallinity of the inorganic phase compared to the organic one was not seen in any of the diffraction peaks from the PANi matrix. However, the zoom plot in Fig. 2d does show some peaks (17.6°, 17.8°, 18.4°, 18.7° and 19.6°) corresponding to the characteristics reported in diffraction peaks for PANi [6].

Mössbauer spectra are shown in Fig. 3. The spectra were fitted using a two sextet model (sextet 1 and 2) for magnetite, $[Fe^{3+}]_A[Fe^{3+}$

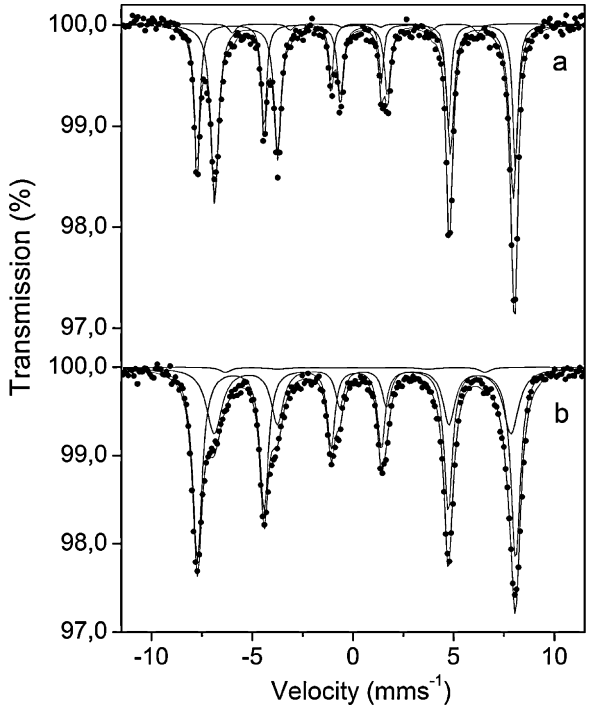

Fig. 3. Mössbauer spectrum. (a) Fe_3O_4, (b) PANi/Fe_3O_4.

Table 2
Hiperfine parameters. Bhf: hyperfine field; δ: isomer shift relative to the isomer shift of α-iron at room temperature.

Sample	Component	Bhf (T)	δ (mm s^{-1})	Area (%)
Fe_3O_4	Sextet 1	49.0	0.16	35.7
	Sextet 2	45.9	0.55	61.4
	Sextet 3	37.7	0.26	2.8
PANi/Fe_3O_4	Sextet 1	48.8	0.17	63
	Sextet 2	45.7	0.49	35
	Sextet 3	38.9	0.29	2

$Fe^{2+}]_B O_4{}^{2-}$. The first sextet corresponded to the Fe^{3+} ions of tetrahedral sites (A sites) and the second sextet corresponded to $Fe^{2.5+}$ ions (Fe^{3+} and Fe^{2+}) from octahedral sites (B sites). Moreover, a sextet of goethite (α-FeOOH) phase (sextet 3) was needed in order to obtain the best fit. As confirmed by XRD, magnetite was incorporated into the PANi phase. The nanocomposite spectra (Fig. 3b) show a marked decrease in the B sites compared to the spectrum for Fe_3O_4, whereas the intensity of A sites (Fe^{3+}) increases. This behavior represents a clear solid-state electronic interaction between magnetite and polyaniline and may be attributed to an electron transfer process from the B sites [Fe^{3+} Fe^{2+}] of Fe_3O_4 to PANi. The partially oxidized Fe^{2+} was converted into Fe^{3+}, later confirmed by UV–vis and CV in solution.

Table 2 shows the hyperfine parameters calculated from Fig. 3. The obtained parameters are in good agreement with those reported for pure magnetite (Bhf1: 49 T, Bhf2: 46 T δ1: 0.15 mm s^{-1}, δ2: 0.56 mm s^{-1}) and goethite (Bhf1: 38.2 T, δ1: 0.25 mm s^{-1}) [29].

The percentage area reported under the curve of the lines of best fit is related to the composition of the obtained materials. According to these spectra and the hiperfine parameters, it is evident that the process for obtaining the PANi/Fe_3O_4 nanocomposite does not interfere significantly with the nature of the oxide. Although rigorous care was taken in the synthesis and purification steps, there was a small amount of α-FeOOH (<3%, sextet 3) found in the oxide phase that could not be detected by XRD, possibly due to its nanometric size and amorphous nature.

TEM images are shown in Fig. 4. Magnetite nanoparticles were found to be cubical shaped with an average size in the order of 80 nm. From Fig. 4b and c, the PANi polymeric phase can be observed as a clear contrast phase, rather than a darker embedded phase corresponding to nanoparticles of Fe_3O_4. From these images a nanocomposite structure can be deduced, mainly made of the aggregation of inorganic nanoparticles surrounded by a PANi matrix. Regarding other methods to obtain nanocomposites, in-situ polymerization has demonstrated to be one of the more efficient techniques to get good polymer–particle interaction. Major properties are improved using this technique mainly due to a higher contact area and lower interphase resistance between the components. This morphology favored the redox interaction, as observed using the Mössbauer spectroscopy.

Fig. 5 shows the Raman spectra of PANi and the nanocomposite recently prepared. The spectrum for PANi displays the characteristic bands of the emeraldine base form. Quinone segments at 1163(β_{C-H}), 1219 (ν_{C-N}), 1470 ($\nu_{C=N}$), and 1592 cm^{-1} ($\nu_{C=C}$) were observed [30]. PANi/Fe_3O_4 showed a characteristic strong band at 667 cm^{-1}, typical of magnetite [31], and a shift in the 1470 cm^{-1} band for the PANi to 1483 cm^{-1} for PANi//Fe_3O_4, likely indicating the interaction of the nanoparticles with the imine nitrogen atoms of the polymer.

To confirm the interaction of nanoparticles with the polymer, UV–vis and CV experiments were then conducted by leaving the nanocomposites under air for 2, 7 and 18 days and running the corresponding measurements.

The optical properties for well dispersed suspensions of PANi and PANi/Fe_3O_4 in DMF are presented in Fig. 6. An absorption band

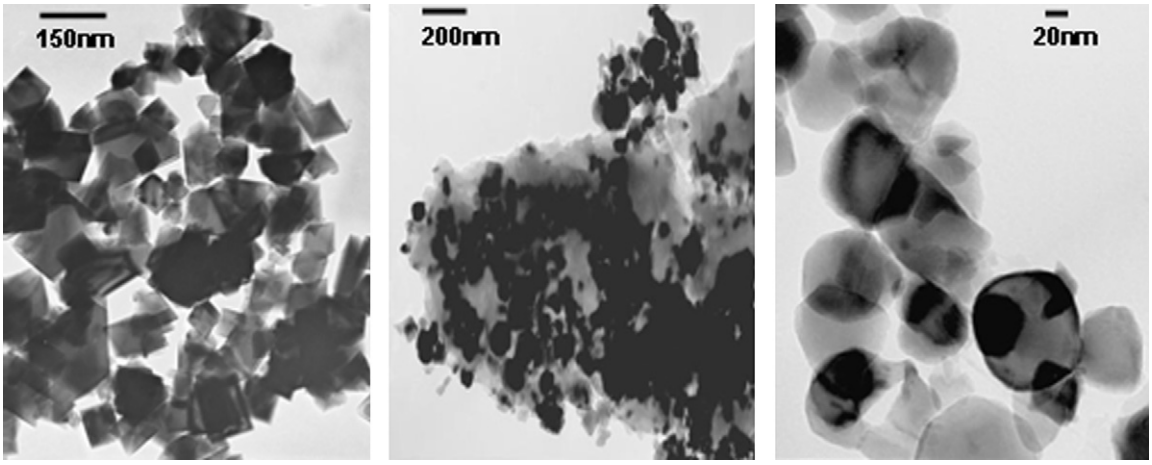

Fig. 4. TEM Images. (a) Fe_3O_4, (b and c) correspond to nanocomposites.

at about 330 nm (see Fig. 6a) corresponding to the π–π* transition of the conjugated polymer can be observed. The broad band observed at 623 nm refers to charge-transfer exciton due to transition from the highest occupied energy level (centered on the benzenoid rings) to the lowest occupied energy level (centered on the quinoid rings) [32]. It can be seen that the π–π* transition is blue-shifted from ~330 nm for pristine PANi to ~323 nm for the PANi/Fe_3O_4 nanocomposite. The absorption band observed at 623 nm for PANi also showed a small blue shift compared to the pristine PANi. These changes are possibly due to a decrease in molecular weight during the polymerization of PANi in the presence of Fe_3O_4, thereby causing a decrease in conjugation, or to redox interactions between both components stabilizing the reduced PANi form. The first hypothesis seems less probable as it is known that nanoparticles can act as nucleation agents or even catalysts in polymerization reactions. This increases the molecular weight of some polymers by lowering the reaction rate, including the propagation, chain transfer, and termination reactions [33].

The evolution of the redox behavior for PANi and the nanocomposite, determined by cyclic voltammetry, is shown in Fig. 7. Three redox transitions can be observed for PANi in the base form (Fig. 7a). The first transition (an oxidation at 0.25 V and a reduction at 0.08 V) corresponds to the inter-conversion from Leucoemeraldine (L) to Emeraldine (E) [34]. A second small redox couple at 0.56 V/0.48 V is associated with the formation of benzoquinone and hydroquinone as additional products from aniline polymerization [35]. The last couple, at 0.76 V/0.65 V, can be related to oxidation from Emeraldine (E) to Pernigraniline (P) [6,35]. Finally, an

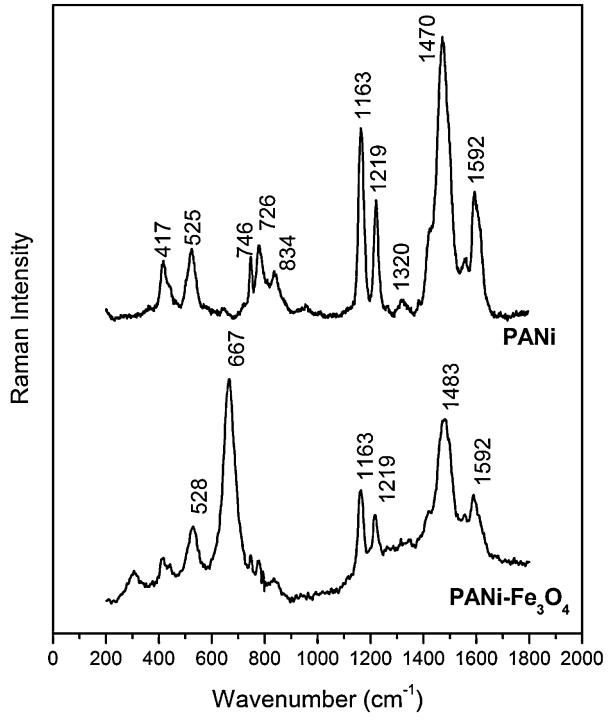

Fig. 5. Raman spectra at day zero. Top: PANi, Bottom: PANi/Fe_3O_4.

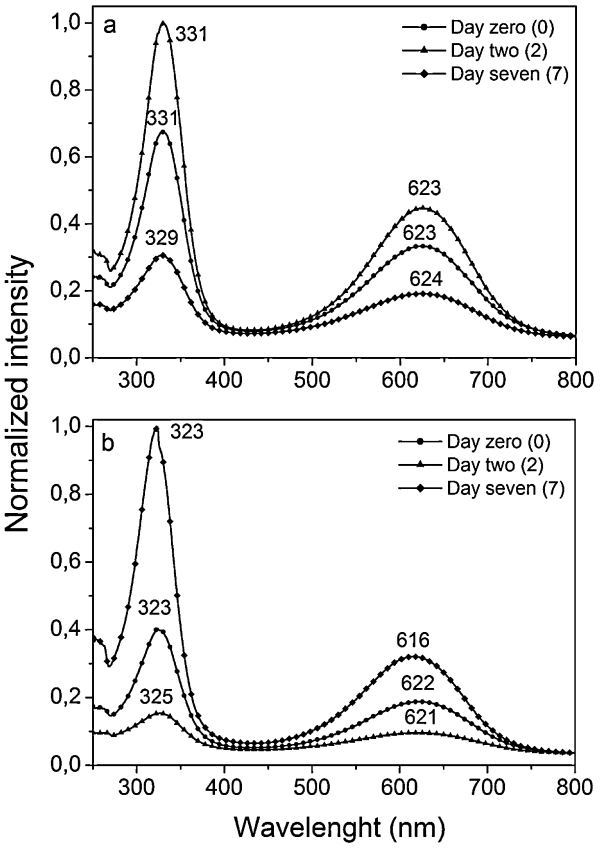

Fig. 6. UV–vis spectra. (a) PANi, (b) nanocomposites.

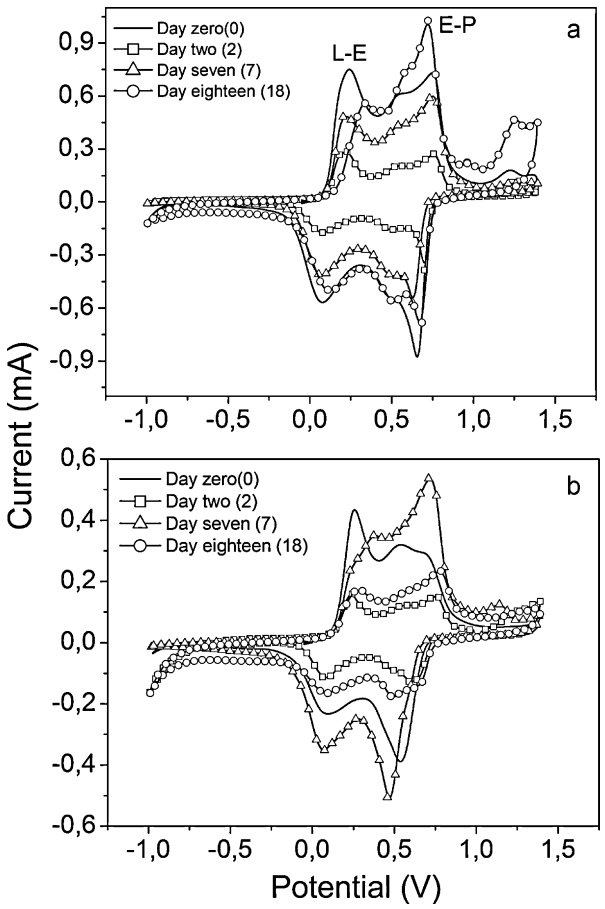

Fig. 7. Cyclic voltammograms in 0.1 M H_2SO_4 with Ag/AgCl as a reference electrode at a scan rate of 10 mV s^{-1}. (a) PANi, (b) PANi-Fe_3O_4.

oxidation peak corresponding to the formation of bipolaron is observed at 1.21 V [34]. It can be seen that for pristine PANi, the E → P transition increases gradually over time in comparison to L → E.

In general the PANi/Fe_3O_4 nanocomposite shows similar transitions to the pristine polymer. However, the peak associated with the L → E transition is greatly enhanced for day zero and is more intense than that found for PANi compared to the band attributed to E → P. The main difference between pristine PANi and the nanocomposite can be recognized over time. As for PANi/Fe_3O_4, an increase in E → P is reached faster (at day seven) than that observed for PANi (at day eighteen), which then decreases at day eighteen stabilizing the E form. Moreover, the E → P transition is clearly shifted to a more anodic potential when the nano-magnetite is incorporated into the polymer. This behavior favors the E phase and makes P phase less probable. The results are in agreement with those observed by Mössbauer spectroscopy, in which an electron from the B sites of magnetite $[Fe^{3+}]_A[Fe^{3+}\ Fe^{2+}]_BO_4{}^{2-}$ can be transferred to the polymer chain and therefore can partially stabilize the Leucoemeraldine/Emeraldine couple, unlike the Emeraldine/Pernigraniline transition.

Finally, the bipolaronic state at 1.21 V is greatly decreased for the nanocomposite, stabilizing the polymer and preventing its oxidation, and demonstrating the advantage of having a partially oxidized inorganic nanoparticle (Fe_3O_4) embedded into PANi. Similar results were found in our previous work where polypyrrole/magnetite films were synthesized by electrochemical methods and the polaronic structure of PPy (benzoid form) is stabilized [22]. Here the decreasing of bipolaronic states suggest stabilization of polaronic forms as intermediate states to finally produced a reduced stabilized form of PANi.

4. Conclusions

From X-ray diffraction analysis and Mössbauer spectroscopy, the formation of a PANi/Fe_3O_4 nanocomposite with the incorporation of magnetite nanoparticles in the PANi matrix was confirmed. Magnetite had a strong redox effect on the electronic properties of the PANi, as the nanoparticles favored the Emeraldine phase. Furthermore, the bipolaronic states of PANi could be dramatically reduced. The nanoparticles/polymer interaction occurred due to the imine nitrogen atoms of the polymer, as observed by RAMAN. The incorporation of Fe_3O_4 nanoparticles into the conductive polymer can greatly enhance its oxidation stability.

Acknowledgment

The authors really appreciate “Programa de Sostenibilidad-UdeA” for supporting this research.

References

[1] H. Liu, X. Hu, J. Wang, R. Boughton, Macromolecules 35 (2002) 9414–9419.
[2] H. Zhou, S. Jiao, J. Chen, W. Wer, Y. Kaung, Thin Solid Films 450 (2004) 233–239.
[3] M. Kanungo, A. Kuamr, A. Contractor, Chem. Mater. 15 (2003) 4658–4665.
[4] W. Li, H. Wang, J. Am. Chem. Soc. 126 (2004) 2278–2279.
[5] P. Khiew, N. Huang, S. Radiman, M. Ahmad, Mater. Lett. 58 (2004) 516–521.
[6] J. Park, S. Park, H. Liu, X. Hu, J. Wang, R. Boughton, A. Koukitu, O. Hatozaki, N. Oyamaa, Synth. Met. 141 (2004) 265–270.
[7] A. Carswell, E. Rear, B. Grady, J. Am. Chem. Soc. 125 (2003) 14793–14800.
[8] X. Shi, A. Briseno, A. Sanidrin, F. Zhou, Macromol. Polyaniline 36 (2003) 4093–4098.
[9] J. Stejskal, P. Kratochvil, A.D. Jenkins, Polymer 37 (1996) 367–369.
[10] D. Zhang, Polym. Test. 26 (2007) 9–13.
[11] J.S. Salafsky, Phys. Rev. B 59 (1999) 10885–10894.
[12] S.J. Su, N. Kuramoto, Synth. Met. 114 (2000) 147–153.
[13] L.J. Zhang, M.X. Wan, J. Phys. Chem. B 107 (2003) 6748–6753.
[14] D.G. Shchukim, I.L. Radtchenko, G.B. Sukhorukov, Mater. Lett. 57 (2002) 1743–1747.
[15] S. Radhakrishnan, S. Prakash, C.R.K. Rao, M. Vijayan, Electrochem. Solid State Lett. 12 (2009) A84–A87.
[16] S.S. Umare, B.H. Shambharkar, R.S. Ningthoujam, Synth. Met. 160 (2010) 1815–1821.
[17] W. Shen, M. Shi, M. Wang, H. Chen, Mater. Chem. Phys. 122 (2010) 588–594.
[18] A.C.V. de Araújo, R.J. de Oliveira, S. Alves Júnior, A.R. Rodrigues, F.L.A. Machado, F.A.O. Cabral, W.M. de Azevedo, Synth. Met. 160 (2010) 685–690.
[19] J.H. Kim, F.F. Fang, H.J. Choi, Y. Seo, Mater. Lett. 62 (2008) 2897–2899.
[20] S. Neves, S.C. Canobre, R.S. Oliveira, C.P. Fonseca, J. Power Sources 189 (2009) 1167–1173.
[21] E.A. Ponzio, T.M. Benedetti, R.M. Torresi, Electrochim. Acta 52 (2007) 4419–4427.
[22] P. Montoya, F. Jaramillo, J. Calderón, S.I. Córdoba de Torresi, R.M. Torresi, Electrochim. Acta 55 (2010) 6116–6122.
[23] B. Jaramillo Tabares, A.A. Zuleta Gil, F. Jaramillo Isaza, Rev. Fac. Ing. Univ. Antioquia 50 (2009) 9–16.
[24] Z. Huang, F. Tang, L. Zhang, Thin Solid Films 471 (2005) p105.
[25] Z.L. Liu, X. Wang, K.L. Yao, G.H. Du, Q.H. Lu, Z.H. Ding, J. Tao, Q. Ning, X.P. Luo, D.Y. Tian, D. Xi, J. Mater. Sci. 39 (2004) 2633.
[26] J. Deng, Ch.L. He, Y. Peng, J. Wang, X. Long, P. Li, A.S.C. Chan, Synth. Met. 139 (2003) 295–299.
[27] MAUD program, http://www.ing.unitn.it/maud/.
[28] R.M. Cornell, U. Schwertmann, Iron Oxide: Structure, Properties, Reactions Ocurrence and Uses, Federal Republic of Germany, Weinheim, 2003.
[29] S. Quillard, G. Louarn, S. Lefrant, A.G. MacDiarmid, Phys. Rev. 50 (1994) 12496–12508.
[30] C.M.S. Izumi, A.M.D.C. Ferreira, V.R.L. Constantino, M.L.A. Temperini, Macromolecules 40 (2007) 3204–3212.
[31] K.G. Neoh, E.T. Kang, K.L. Tan, Polymer 34 (1993) 3921–3928.
[32] G.G. Wallace, G.M. Spinks, L.A.P. Kane-Maguire, P.R. Teasdale, Conductive Electroactive Polymers: Intelligent Materials Systems, second ed., CRC Press LLC, 2003.
[33] Q. Wang, Z. Zhou, L. Song, H. Xu, L. Wang, J. Polym. Sci. Part A 42 (2004) 38–43.
[34] W.-Ch. Chen, T.-Ch. Wen, A. Gopalan, Synth. Met. 128 (2002) 179–189.
[35] A. Abd-Elwahed, R. Holze, Synth. Met. 131 (2002) 61–70.